JOURNAL OF SPACECRAFT AND ROCKETS
Vol. 43, No. 5, September–October 2006

Engineering Notes

ENGINEERING NOTES are short manuscripts describing new developments or important results of a preliminary nature. These Notes should not exceed 2500 words (where a figure or table counts as 200 words). Following informal review by the Editors, they may be published within a few months of the date of receipt. Style requirements are the same as for regular contributions (see inside back cover).

Active Vibration Isolation of Rigid Body Using a Pneumatic Octostrut Platform

Q. J. Yang*
Harbin Institute of Technology, 150001 Harbin, People's Republic of China
G. T. Zheng†
Tsinghua University, 100084 Beijing, People's Republic of China
and
W. H. Huang‡
Harbin Institute of Technology, 150001 Harbin, People's Republic of China

DOI: 10.2514/1.23053

I. Introduction

ACTIVE control has recently been developed as a method to isolate a spacecraft from the launch vehicle in effort to overcome the following drawbacks of a passive octostrut platform found in [1]: 1) the low frequency resonances introduced into the system; 2) the conflict between lower isolation frequency and stiffness high enough to limit quasi-static stroke and avoid possible collision between the spacecraft and fairing; and 3) different requirements in stiffness for different directions. An active octostrut isolation platform as shown in Fig. 1 is proposed, and widely used pneumatic springs [2] are used as its active actuators for their cleanness and long stroke. The payload selected for this research is a rigid body because the first natural frequency is usually fairly high for many small spacecraft. Different from centralized, overlapped, or decentralized control strategies [3–5], a grouped control strategy based on minimal two-norm redundancy solution is adopted after a careful study of the inherent characteristics of the octostrut platform.

II. System Modeling

Two Cartesian coordinate systems, $o_t x_t y_t z_t$ for the payload and $o_b x_b y_b z_b$ for the base, are established at the centers of the two connection joint planes. The generalized displacements of the base are $\boldsymbol{x}_b = [z_b \gamma_b x_b \beta_b y_b \alpha_b]$, and those of the payload are $\boldsymbol{x}_t = [z_t \gamma_t x_t \beta_t y_t \alpha_t]$. The generalized forces acting on the payload are $\boldsymbol{f}_t = [f_z^t \tau_\gamma^t f_x^t \tau_\beta^t f_y^t \tau_\alpha^t]$.

Received 8 February 2006; revision received 28 May 2006; accepted for publication 29 May 2006.

*Associate Professor, Department of Space Engineering and Applied Mechanics, School of Mechatronics Engineering; yqj@hit.edu.cn.

†Professor, School of Aerospace, Tsinghua University; gtzhengtu@yahoo.co.uk.

‡Professor, Department of Space Engineering and Applied Mechanics, School of Astronautics; whhuang@hit.edu.cn

The platform has eight struts and eight valves, and by assuming all the struts and valves have the same characteristics, we can model them by

$$\dot{\boldsymbol{p}} = k_1 \boldsymbol{u} - \omega_p \boldsymbol{p} - A^{-1} k_p \dot{\boldsymbol{l}} \tag{1}$$

where $\boldsymbol{u}$ is the control input vector, $\boldsymbol{p}$ is the pressure in the pneumatic chamber, k_1 is the gain coefficient matrix, ω_p is the corner frequency of the pneumatic spring, A is the effective section area of the pneumatic spring, k_p is the pneumatic spring stiffness, and $\boldsymbol{l}$ is the length of the strut. Strut force $\boldsymbol{f}_1$ consists of mechanical spring force, damping force, and pneumatic force, and it can be expressed as

$$\boldsymbol{f}_1 = \mathbf{K}\Delta\boldsymbol{l} + \mathbf{C}\dot{\boldsymbol{l}} + A\boldsymbol{p} \tag{2}$$

$$\Delta\boldsymbol{l} = \mathbf{L}_b \boldsymbol{x}_b + \mathbf{L}_t \boldsymbol{x}_t \tag{3}$$

where $\mathbf{K}$ is the stiffness matrix, $\mathbf{C}$ is the damping force coefficient matrix, $\mathbf{L}_b$ is the gain matrix of $\Delta\boldsymbol{l}$ over $\boldsymbol{x}_b$, $\mathbf{L}_t$ is the gain matrix of $\Delta\boldsymbol{l}$ over $\boldsymbol{x}_t$, $\boldsymbol{x}_b$ is the generalized displacement of the base, and $\boldsymbol{x}_t$ is the generalized displacement of the payload.

The eight struts provide the payload with the following generalized force $\boldsymbol{f}_t$:

$$\boldsymbol{f}_t = \mathbf{F}\boldsymbol{f}_1$$

$$\mathbf{F} = \frac{\partial \boldsymbol{f}_t}{\partial \boldsymbol{f}_1} = \begin{bmatrix} f_{c3} & f_{c3} & f_{c3} & f_{c3} & f_{c3} & f_{c3} & f_{c3} & f_{c3} \\ f_{c6} & -f_{c6} & f_{c6} & -f_{c6} & f_{c6} & -f_{c6} & f_{c6} & -f_{c6} \\ f_{c1} & f_{c2} & -f_{c2} & -f_{c1} & -f_{c1} & -f_{c2} & f_{c2} & f_{c1} \\ f_{c2} & f_{c1} & f_{c1} & f_{c2} & -f_{c2} & -f_{c1} & -f_{c1} & -f_{c2} \\ -f_{c4} & -f_{c5} & -f_{c5} & -f_{c4} & f_{c4} & f_{c5} & f_{c5} & f_{c4} \\ f_{c5} & f_{c4} & -f_{c4} & -f_{c5} & -f_{c5} & -f_{c4} & f_{c4} & f_{c5} \end{bmatrix} \tag{4}$$

The following are the expressions of elements in matrix $\mathbf{F}$:

$$f_{c1} = \frac{r_b \cos\theta_b - r_t \cos\theta_t}{l_0}, \qquad f_{c2} = \frac{r_b \sin\theta_b - r_t \sin\theta_t}{l_0}$$

$$f_{c3} = \frac{h}{l_0}, \qquad f_{c4} = \frac{h r_t \sin\theta_t}{l_0}, \qquad f_{c5} = \frac{h r_t \cos\theta_t}{l_0}$$

$$f_{c6} = \frac{f_{c1} r_t \sin\theta_t - f_{c2} r_t \cos\theta_t}{l_0}$$

where the parameters r_b, r_t, θ_b, and θ_t are as shown in Fig. 1, h is the height difference of upper and lower joint planes, and l_0 is the initial length of the strut.

The kinetic equation of the payload is

$$\boldsymbol{f}_t + \boldsymbol{f} = \mathbf{M}\ddot{\boldsymbol{x}}_t \tag{5}$$

where $\mathbf{M}$ is the inertia matrix and $\boldsymbol{f}$ is the disturbance force vector.

By combining Eqs. (1–5) together and denoting

$$\mathbf{D}(s) = \mathbf{M}s^3 + (\mathbf{M}\omega_p + \mathbf{FCL}_t)s^2 + \mathbf{F}(k_p\mathbf{I} + \omega_p\mathbf{C} + \mathbf{K})\mathbf{L}_t s + \omega_p \mathbf{FKL}_t$$

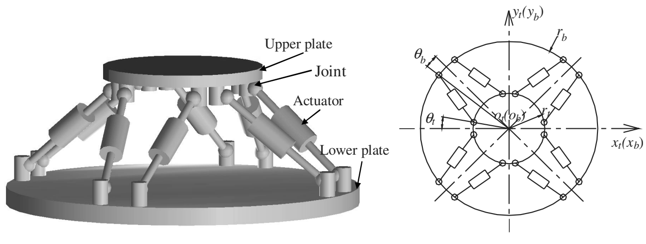

a) Stereogram b) Top-view

Fig. 1 Mechanical structure of an octostrut platform.

and

$$\mathbf{N}(s) = \mathbf{FCL}_b s^2 + \mathbf{F}(k_p\mathbf{I} + \omega_p\mathbf{C} + \mathbf{K})\mathbf{L}_b s + \omega_p\mathbf{FKL}_b$$

the complete model can be established as

$$\mathbf{D}(s)\boldsymbol{x}_t = \mathbf{N}(s)\boldsymbol{x}_b + Ak_1\mathbf{F}\boldsymbol{u} + (s + \omega_p)\boldsymbol{f} \tag{6}$$

Calculations show that both $\mathbf{D}(s)$ and $\mathbf{N}(s)$ have the same structure of

$$\begin{bmatrix} * & & & & & \\ & * & & & & \\ & & * & * & & \\ & & * & * & & \\ & & & & * & * \\ & & & & * & * \end{bmatrix}$$

wherein the asterisks represent nonzero elements. It means that the passive isolation system could be divided into four uncoupled subgroups: z_t/z_b as subgroup 1, γ_t/γ_b as subgroup 2, x_t and β_t over x_b and β_b as subgroup 3, and y_t and α_t over y_b and α_b as subgroup 4. This results from the symmetrical structure of the octostrut platform.

III. Design of Controller

The design of a controller as shown in Fig. 2 starts with a redundancy solution followed by stiffness control and transmissibility control. After converting the stiffness increment matrix into a strut length feedback gain matrix, strut length can be used in stiffness control instead of generalized displacements. According to the way of decomposing the passive isolation system, transmissibility control is divided into four uncoupled subgroups.

While it is assumed that $\tilde{\boldsymbol{u}}$ is the generalized control input and $\boldsymbol{u}_1$ is the real control input, the equation

$$Ak_1\mathbf{F}\boldsymbol{u}_1 = \tilde{\boldsymbol{u}} \tag{7}$$

holds, and its minimal two-norm solution is

$$\boldsymbol{u}_1 = A^{-1}k_1^{-1}\mathbf{B}\tilde{\boldsymbol{u}} \tag{8}$$

where

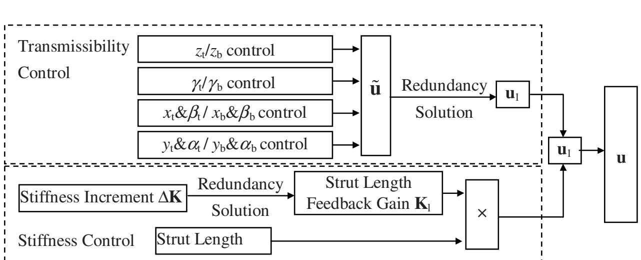

Fig. 2 Block diagram of the controller.

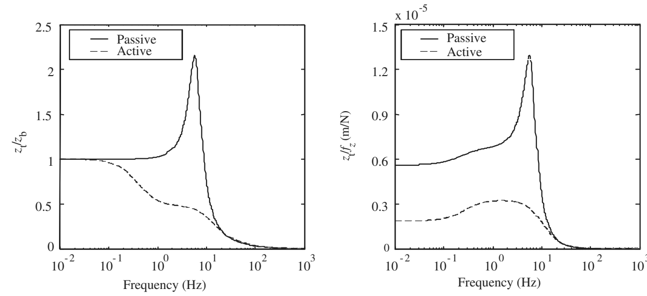

a) b)

Fig. 3 z_t transmissibility and receptiveness.

$$\mathbf{B} = \mathbf{F}^+ = \begin{bmatrix} b_1 & b_1 & b_1 & b_1 & b_1 & b_1 & b_1 & b_1 \\ b_2 & -b_2 & b_2 & -b_2 & b_2 & -b_2 & b_2 & -b_2 \\ b_3 & b_4 & -b_4 & -b_3 & -b_3 & -b_4 & b_4 & b_3 \\ b_5 & b_6 & -b_6 & -b_5 & -b_5 & -b_6 & b_6 & b_5 \\ b_4 & b_3 & b_3 & b_4 & -b_4 & -b_3 & -b_3 & -b_4 \\ -b_6 & -b_5 & -b_5 & -b_6 & b_6 & b_5 & b_5 & b_6 \end{bmatrix}^T \tag{9}$$

and the elements in matrix $\mathbf{B}$ are

$$b_1 = \frac{l_0}{8h}, \qquad b_2 = \frac{l_0}{8r_b r_t \sin(\theta_t - \theta_b)}, \qquad b_3 = \frac{-l_0 \sin\theta_t}{4r_b \sin(\theta_b - \theta_t)}$$
$$b_4 = \frac{l_0 \cos\theta_t}{4r_b \sin(\theta_b - \theta_t)}, \qquad b_5 = \frac{l_0(r_b \sin\theta_b - r_t \sin\theta_t)}{4hr_t r_b \sin(\theta_b - \theta_t)}$$
$$b_6 = \frac{-l_0(r_b \cos\theta_b - r_t \cos\theta_t)}{4hr_t r_b \sin(\theta_b - \theta_t)}$$

While it is assumed that $\Delta\mathbf{K}$ is the stiffness increment and $\mathbf{K}_1$ is the strut length feedback gain matrix, the following equation holds:

$$\omega_p^{-1}\mathbf{K}_1\mathbf{L}_t = \Delta\mathbf{K} \tag{10}$$

Because $\mathbf{L}_t$ is dual with $\mathbf{F}$, i.e., $\mathbf{L}_t = \mathbf{F}^T$, the solution for Eq. (10) is then

$$\mathbf{K}_1 = \omega_p \Delta\mathbf{K}\mathbf{B}^T \tag{11}$$

Because the highest order of the $\mathbf{D}(s)$ matrix is 3, $\tilde{\boldsymbol{u}}$ can be constructed as

$$\tilde{\boldsymbol{u}} = -\mathbf{K}_v\dot{\boldsymbol{x}}_t - \mathbf{K}_a\ddot{\boldsymbol{x}}_t \tag{12}$$

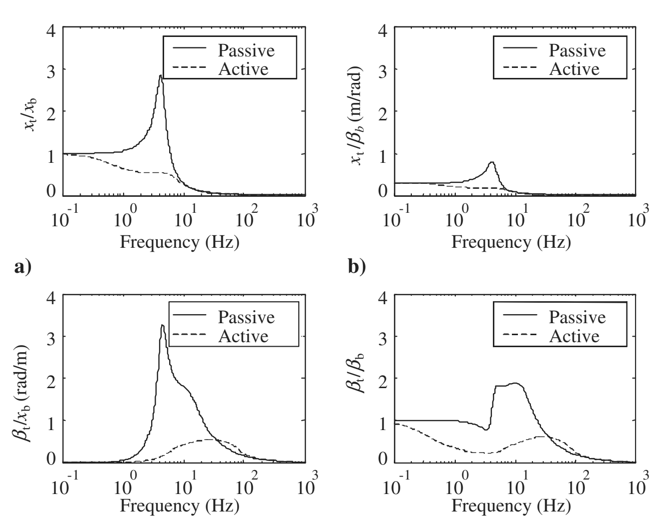

a) b) c) d)

Fig. 4 Transmissibility of $\boldsymbol{x}_t$ and $\boldsymbol{\beta}_t$ over $\boldsymbol{x}_b$ and $\boldsymbol{\beta}_b$.

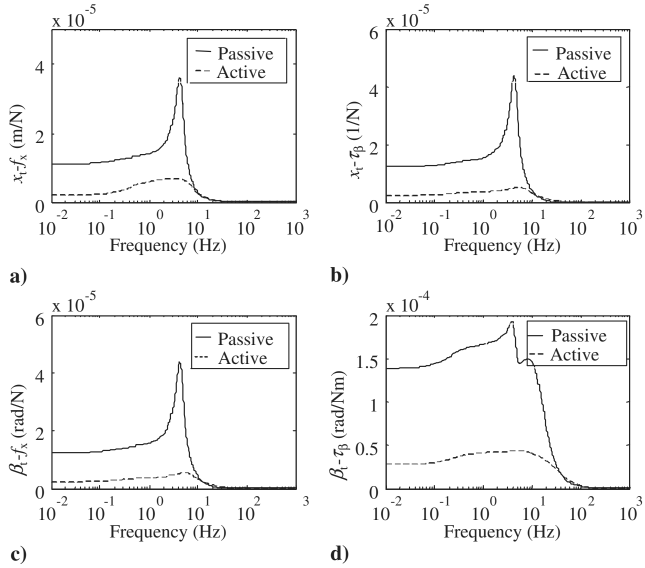

Fig. 5 Dynamic receptiveness of x_t and β_t over f_x and τ_β.

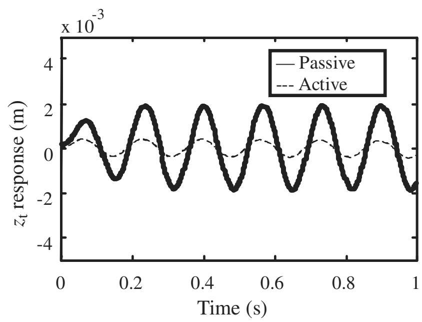

Fig. 6 z_t responses under z_b excitation.

where $\mathbf{K}_v$ is the payload velocity feedback gain matrix and $\mathbf{K}_a$ is the payload acceleration feedback gain matrix.

The structures selected for $\Delta\mathbf{K}$, $\mathbf{K}_v$, and $\mathbf{K}_a$ are the same as the structure of $\mathbf{D}(s)$ and $\mathbf{N}(s)$, and so the closed-loop system can still be divided into four uncoupled subsystems. The determination of $\mathbf{K}_v$ and $\mathbf{K}_a$ is thus greatly simplified.

The passive and active transmissibility of z_t over z_b and the direct dynamic receptance of payload are as shown in Fig. 3. It can be seen from them that active control eliminates the resonance of the passive system and makes the isolation frequency in the z_t direction of the passive system decrease from above 6 Hz to less than 0.1 Hz, and it reduces the steady-state receptiveness to $1/3$ of the passive one, which means an increase in stiffness up to 3 times.

The transmissibility and dynamic receptiveness of subgroup 3 are shown in Figs. 4 and 5 respectively. It can be seen from them that, with active control, the whole transmissibility is less than 1 and the isolation frequencies are much lower than those of passive case; and different from that in the z_t direction, the stiffness increases up to about 5 times here, which means that active control can meet different stiffness requirements in different directions.

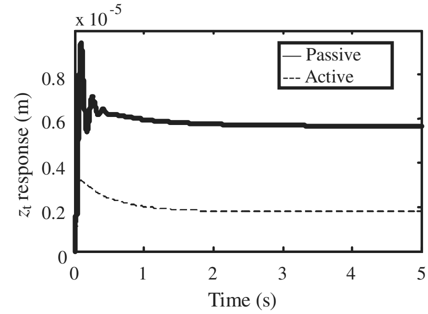

Fig. 7 z_t responses under f_z excitation.

Time domain simulations are made to verify the effectiveness of the controller. The responses of z_t under z_b excitation of 0.001 mm and 6 Hz, both with and without control, are as shown in Fig. 6, and those under unit force excitation acting on the upper plate are shown in Fig. 7. It can be seen from Fig. 6 that the active responses of the payload drop even below excitation input, which means passive resonances are eliminated and the isolation band is broaden by active control. It can be seen from Fig. 7 that the stiffness in z_t increases up to about 3 times the passive one, and the damping ratio is better.

IV. Conclusion

It can be concluded from the preceding theoretical analyses and simulation results that high steady stiffness and lower isolation frequency can be simultaneously acheived by active control because 1) an analytical minimal norm redundancy has been identified; 2) steady stiffness can be increased greatly by strut length feedback; 3) resonance peaks can be eliminated and the isolation frequencies can be reduced significantly by payload velocity and acceleration feedback; and 4) grouped control strategy proposed in accordance with the characteristics of the system simplifies the design of a controller without sacrificing its control performance.

References

[1] Liu, L. K., Liang, L., Zheng, G. T., Huang, W. H., "Dynamic Design of Octostrut Platform for Launch Stage Whole-Spacecraft Vibration Isolation," *Journal of Spacecraft and Rockets*, Vol. 42, No. 4, 2005, pp. 654–662.

[2] Kienholz, D. A., "Active Alignment and Vibration Control System for a Large Airborne Optical System," *Proceedings of SPIE*, Vol. 3989, March 2000, pp. 464–471.

[3] Kim, S.-M., Elliott, S. J., and Brennan, M. J., "Decentralized Control for Multi-Channel Active Vibration Isolation," *IEEE Transactions on Control Systems Technology*, Vol. 9, No. 1, 2001, pp. 93–100.

[4] Brennan, M. J., Elliott, S. J., and Huang, X., "Active Vibration Isolation Using Decentralized Velocity Feedback Control," *Proceedings of SPIE*, Vol. 4763, March 2003, pp. 119–126.

[5] Iftar, A., "Decentralized Estimation and Control with Overlapping Input, State, and Output Decomposition," *Automatica*, Vol. 29, No. 2, 1993, pp. 511–516.

L. Peterson
Associate Editor